

Original Article

Ligustrazine reverts anthracycline chemotherapy resistance of human breast cancer by inhibiting JAK2/STAT3 signaling and decreasing fibrinogen gamma chain (FGG) expression

Yu-Lin Liu¹, Ze-Xuan Yan², Yu Xia¹, Xiao-Ye Xie³, Kai Zhou², Li-Li Xu¹, Yan-Long Shi³, Qiang Wang^{1,3}, Jing-Wang Bi³

¹Clinical Laboratory, Navy 971 Hospital of PLA, Qingdao 266071, China; ²Institute of Pathology and Southwest Cancer Center, Southwest Hospital, Army Medical University, Chongqing 400038, China; ³Department of Oncology, 960 Hospital of PLA, Jinan 250031, China

Received September 29, 2019; Accepted February 7, 2020; Epub March 1, 2020; Published March 15, 2020

Abstract: Chemotherapy resistance is a major challenge for breast cancer treatment. It is necessary to elucidate the mechanisms of anthracycline resistance to develop new chemosensitizers for breast cancer. In this study, we explored the effects of ligustrazine (TMP) on reverting anthracycline resistance of breast cancer cells, as well as its related mechanisms. Clinical significance of fibrinogen gamma chain (FGG) expression was also analyzed in breast cancer tissues. We provided evidence that breast tumor cell derived FGG participated in anthracycline chemoresistance of breast cancer. Further, TMP reverted epirubicin resistance by inhibiting JAK2/STAT3 signaling and decreasing FGG expression. Meanwhile, the elimination of cancer stem cell was observed in TMP treated chemoresistant breast cancer cells. Clinical analysis demonstrated that patients with FGG expressing breast cancer showed a dramatically low response to anthracycline-based chemotherapy and poor survival. Our data collectively indicated that FGG was an independent detrimental factor for anthracycline based chemotherapy for breast cancer patients. TMP was a novel chemosensitizer for FGG-induced anthracycline chemoresistance in breast cancer treatment.

Keywords: Ligustrazine, fibrinogen gamma chain, breast cancer, JAK2/STAT3 pathway, anthracycline, chemotherapy resistance

Introduction

Therapeutic resistance is among the major challenges for breast cancer patients, which led to secondary metastasis and recurrence [1]. Genotoxic chemotherapy, including anthracycline, is an effective therapy in clinical practice. Epirubicin (EPI) is a principal approached anthracycline for breast cancer, which induced irreparable DNA damage for therapeutic effects [2]. However, intrinsic and secondary chemoresistance enhanced DNA repair to attenuate treatment response [3]. It is necessary to elucidate the regulation mechanisms of chemosensitivity and drug resistance to develop new chemosensitizers for breast cancer.

Ligustrazine (2,3,5,6-tetramethylpyrazine, TMP) is the major constituent of *Rhizoma Chuanxiong*. TMP exhibits a strong anti-oxidative activity,

which was widely used in the treatment of cerebral and cardiac ischemic diseases for decades [4]. Recent studies indicated that TMP inhibited tumor metastasis and angiogenesis *in vivo* and *in vitro* by inducing cell apoptosis [5]. Previous studies also supported that TMP is an ameliorated effect on chemotherapy and reverting multidrug resistance [6, 7], which was a promising option for improving anthracycline-based chemosensitivity of breast cancer.

Accumulated evidences have suggested that plasma fibrinogen, an acute phase glycoprotein, is an important factor during cancer progression [8]. Fibrinogen is a large plasma protein composed of two sets of α , β and γ chains, which are encoded by independent genes [9]. Elevated pretreatment plasma fibrinogen is an independent detrimental predictor for patients with solid tumors [10]. Previous studies have

Ligustrazine reverts breast cancer anthracycline chemoresistance

indicated that TMP attenuated blood hypercoagulable state by reducing fibrinogen levels, whereas the underlying molecular mechanisms have not been fully elucidated yet.

In this study, we provided evidence that tumor cells derived fibrinogen gamma chain (FGG) participated in anthracycline chemoresistance of breast cancer. Furthermore, TMP reverted EPI resistance by inhibiting Janus kinase (JAK)/signal transducer and activator of transcription (STAT) signaling and decreasing FGG expression. Meanwhile, the elimination of cancer stem cells was also observed in TMP treated chemoresistant cancer cells. We demonstrated that patients with FGG expressing tumor showed a dramatically weak response to anthracycline-based chemotherapy. Our study collectively revealed TMP as a novel chemosensitizer for FGG-induced anthracycline chemoresistance in breast cancer treatment.

Materials and methods

Human primary tumor samples and clinical information

Breast cancer tissue samples and clinical document were collected from 405 patients were collected from 2006 to 2008. All patients received EPI-based chemotherapy after surgery. Clinical information and follow-up data, including preoperative serum fibrinogen levels, were collected and analyzed as previous report [11]. Criteria for anthracycline resistance were defined as recurrence, metastasis or death occurred within three years after anthracycline-based chemotherapy treatment.

Cell culture

Human breast cancer cell lines MCF7 and T47D were obtained from American Type Culture Collection (ATCC, MD). Both cells were grown in Dulbecco's Modified Eagle Medium contained 1% penicillin and streptomycin, supplemented with 10% fetal bovine serum. EPI and TMP were obtained from Sigma-Aldrich (St Louis, MO). EPI resistant MCF7/EP cells were maintained in DMEM medium with gradient elevated EPI, which was continuous passage cultured for six months.

Cell infection

FGG plasmid was a gift from Gavin Wright (Addgene plasmid # 52031). Flag-tagged con-

stitutively activated STAT3 (STAT3-C) plasmids were constructed as previous report [12]. Cell infection was performed with fresh lentivirus-containing medium supplemented with 8 µg/ml polybrene. The infection efficiency was confirmed with Western blot assays.

Western blot analysis

Western blot assays were performed as our previous study [13]. Primary antibodies, including FGG (ab217783), cleaved PARP (ab32064), Bcl-2 (ab32124), Bcl-XL (ab32370), JAK2 (ab108596), p-JAK2 (Y1007, 1008, ab32101), STAT3 (ab119352), p-STAT3 (S727, ab32143), Oncostatin M (ab133748), anti-Flag (ab49763) and β-actin (ab8226) were purchased from Abcam (Cambridge, MA).

Quantitative real-time PCR (qRT-PCR)

qRT-PCR assays were performed as previous study [13]. RNAzol reagent were purchased from Invitrogen (Carlsbad, CA). The primers sequences of FGG: Forward 5'-GAATTTGGC-TGGGAAATGA-3'. Reverse 5'-ATCATCGCCAAA-TCAAAG-3'.

Cell viability assays

Cell viability assays were performed as previous report [13]. Cell proliferation was measured with a WST-8 kit (Beyotime Inst Biotech, Shanghai, China) according to manufacturer's instructions. The absorbance at 450 nm was measured with Multiskan Spectrum 1500 (Thermo Scientific, PA). IC₅₀ (50% cell growth inhibition) was analyzed with Prism GraphPad 8.0 (GraphPad Inc., La Jolla, CA).

Colony formation assays

Single-cell suspensions were cultured in DMEM medium with indicated TMP or equal vehicle combined with 2.2 µg/mL EPI in 12-well plates (200 cells/well) for two weeks. Cell clones were fixed and stained with crystal violet. Clones with more than 50 cells were counted with microscope. Three independent assays were performed.

Xenografts

Subcutaneous xenografts were established as our previous study [13]. Totally 10⁶ breast cancer cells were subcutaneous planted until 100 mm³. The mice were randomly separated into

Ligustrazine reverts breast cancer anthracycline chemoresistance

two groups for TMP treatment. TMP (100 mg/kg/d) or vehicle control was administered intraperitoneally every other day. The animal experiments were conformed to the Declaration of Helsinki (revised in Fortaleza, Brazil, October 2013) and approved by the Ethics Committee of Animal Care and Use Committee of Army Medical University.

Cell apoptosis analysis

Cell apoptosis was measured with Annexin V-FITC Apoptosis Detection Kit (Beyotime Ins. Shanghai, China). Typically, harvested cells were stained with Annexin V and propidium iodide in 100 μ l binding buffer for 30 min in dark room. Then tested with FACS Aria II flow cytometer (BD Biosciences, NJ).

Caspase-3 activity measurement

Caspase-3 Activity Assay Kit (Beyotime Ins. Biotec, China) was used to determine Caspase-3 activity. TMP treated cells were lysed and incubated with 200 μ M DEVD-pNA substrate at 37°C for 1 h. Then we measured the absorbance at 405 nm with microplate reader (Thermo Electron Corporation, MA).

Mammosphere formation assays

Single-cell suspension of MCF7/EP cells (500 cells/well) were seeded in ultralow attachment plate (Corning Inc, Corning, NY) with conditioned DMEM/F-12 medium as previous studies [13]. Mammospheres were counted manually after 7 days culture. Then mammosphere cells were collected and suspended for secondary sphere formation.

Flow cytometry for ALDH1 percentage

Flowcytometry analysis for ALDH1 was measured with The ALDEFLUOR kit (StemCell Technologies, Durham, NC) in FACS Aria II flow cytometer (BD Biosciences, San Jose, CA) as previous study [13]. Then analyzed with FlowJo software (Tree Star, San Carlos, CA).

Immunohistochemical staining (IHC)

Human tumor and xenograft specimens were prepared for sections. IHC staining was conducted with Ventana Discovery XT automated staining system (Ventana Medical System,

Inc., Tucson, AZ) following the manufacturers' protocols as previous report [14]. FGG (ab217783), Bcl-2 (ab32124), Ki67 (ab92742), ALDH1A1 (ab215996) and p-STAT3 (S727, ab32143) primary antibody was purchased from Abcam.

Statistical analysis

Statistical analyses were performed with IBM SPSS statistics 24.0 (IBM, Chicago, IL), Graphpad Prism 8.0 (GraphPad Software, Inc., La Jolla, CA). Data from at least three independent experiments are described as the means \pm standard deviation (SD). Student's t-tests were used to compare the differences between groups. Fisher's exact test was used to assess the clinical correlation. Cox proportional-hazards regression was used for univariate and multivariate analysis. Kaplan-Meier analysis and log-rank test were used for prognostic values. All statistical tests were two-sided, and $P \leq 0.05$ was considered statistically significant.

Results

Increased FGG levels are correlated with anthracycline chemotherapy resistance in breast cancer

We evaluated the correlation of serum fibrinogen levels and chemotherapy response with anthracycline based chemotherapy in human breast cancer. Preoperative serum fibrinogen levels were estimated in 405 breast cancer patients that received anthracycline chemotherapy. Our results indicated that the patients with high preoperative fibrinogen levels (> 3.00 g/L) exhibited high percentage of anthracycline chemotherapy resistance than those with low fibrinogen levels (36.84% vs. 12.65%. $P < 0.001$. **Figure 1A**). Moreover, the patients resistant to anthracycline based chemotherapy showed higher fibrinogen levels than those effective ones ($P < 0.001$. **Figure 1B**). Further analysis was performed for the tumor-derived fibrinogen chains with TCGA data (1088 cases), including FGA, FGB and FGG. The results supported that breast tumor tissues were important source for plasm fibrinogen. Totally, 968 tumor specimens have at least one chain of fibrinogen mRNA expression (89.0%). Among them, 439 specimens were positive for FGA mRNA (40.3%), 675 for FGB (62.0%) and 678

Ligustrazine reverts breast cancer anthracycline chemoresistance

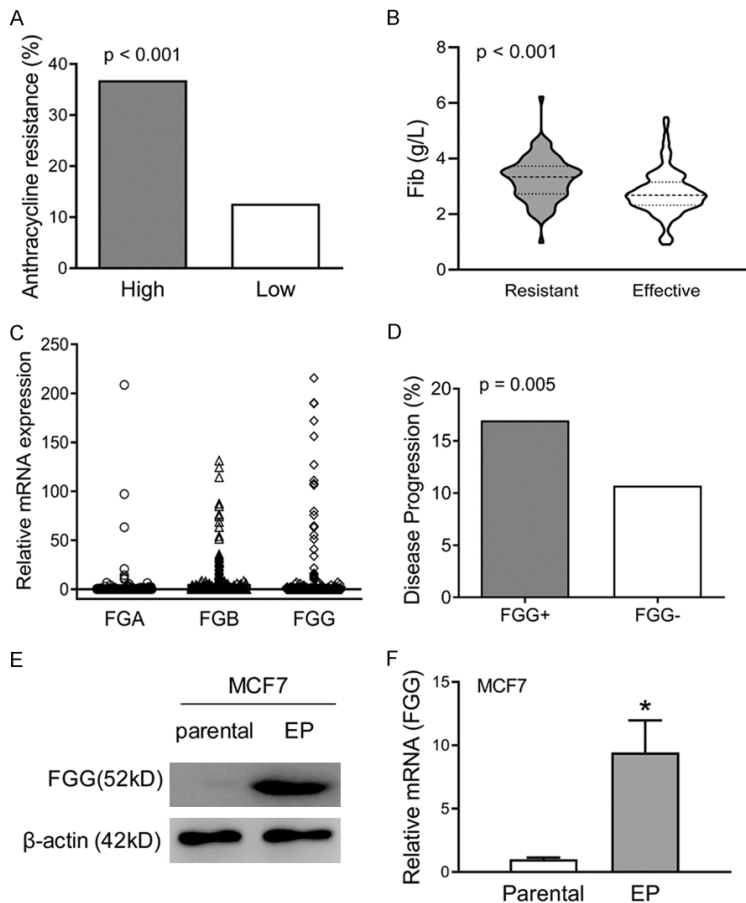


Figure 1. Increased FGG levels are correlated with anthracycline chemotherapy resistance in breast cancer. **A.** Preoperative serum fibrinogen levels were collected from 405 breast cancer patients. The patients with high fibrinogen levels (> 3.00 g/L) showed higher percentage of anthracycline chemotherapy resistance than low fibrinogen patients ($P < 0.001$). **B.** The anthracycline based chemotherapy resistant patients showed higher fibrinogen levels than those effective ones ($P < 0.001$). **C.** The mRNA levels of FGA, FGB and FGG, three isolate chains of fibrinogen, were analyzed in 1088 breast cancer tissues from TCGA data. **D.** The comparison of disease progression was analyzed between FGG-positive patients and negative patients with TCGA data. Increased disease progression was observed in the patients with positive FGG mRNA expression. $P = 0.005$. **E.** The protein level of FGG were measured in EPI resistant MCF7 cells (MCF7/EP vs. parental) with Western blot assays. β -actin was used as loading control. **F.** Comparison of FGG mRNA levels between MCF7/EP vs. parental cells, which was determined by qRT-PCR assays. β -actin was used as control.

for FGG (62.3%) (**Figure 1C**). Furthermore, increased FGG mRNA expression was correlated with increased disease progression after surgery (**Figure 1D**). Based on these results, an EPI resistant MCF7 cells, MCF7/EP, was prepared for the correlation of FGG and anthracycline resistance. Elevated FGG protein levels were observed in MCF7/EP cells than parental ones by Western blot assays (**Figure 1E**). The mRNA abundance was consistent with the protein levels (**Figure 1F**), indicating the promising

role of FGG in anthracycline-based chemotherapy resistance of breast cancer cells.

FGG promotes breast cancer cell survival and proliferation with anthracycline treatment in vitro and in vivo

Exogenous expression of FGG in breast cancer cell lines were confirmed by immunoblotting assays (**Figure 2A**). Notably, MCF7-FGG cells showed significant higher IC₅₀ under EPI treatment than control cells (IC₅₀: $9.32 \mu\text{M}$ vs. $3.23 \mu\text{M}$, $P < 0.01$, **Figure 2B**). Furthermore, CCK-8 assays showed that cell viability was significantly increased in MCF7-FGG cells than control ones with $3.0 \mu\text{M}$ EPI treatment (**Figure 2C**). Increased cell viability was observed in FGG overexpressed T47D cells (**Figure 2D**). Our results also indicated that cell clone formation of FGG overexpressing cells was increased than control cells with EPI treatment (**Figure 2E, 2F**). More importantly, xenografts of infected MCF7 cells were subcutaneously planted in nude mice, and then, we treated the mice with EPI medium (5 mg/kg EPI per 2 days). The xenografts of MCF7-FGG cells showed significantly increased tumor volume and weight than control cells (**Figure 2G, 2H**). These data suggested that FGG was involved

in anthracycline chemotherapy resistance of breast cancer.

TMP reduces FGG expression and reverses anthracycline resistance of breast cancer cells

TMP was used as a fibrinogen regulator to ameliorate hypercoagulable state [15]. Then, we evaluated TMP as a chemosensitizer in anthracycline resistant breast cancer cells. As expected, TMP treatment significantly reduced the expression levels of FGG in a dose-dependent

Ligustrazine reverts breast cancer anthracycline chemoresistance

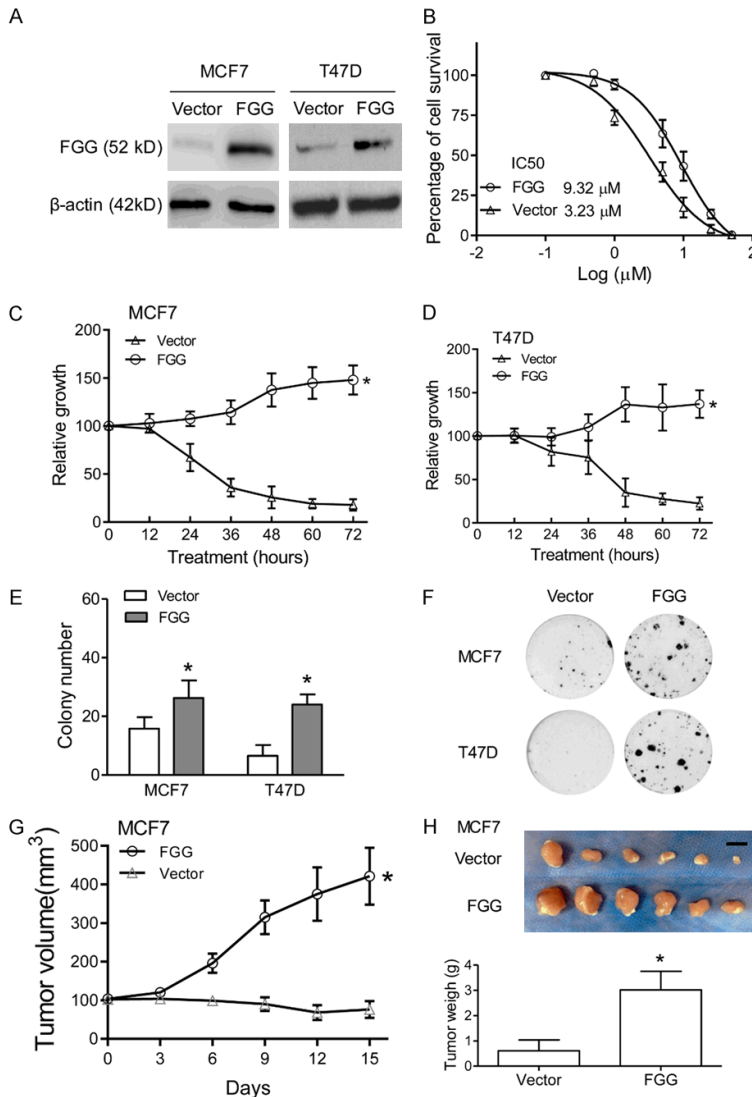


Figure 2. FGG promotes breast cancer cell survival and proliferation with anthracycline treatment *in vitro* and *in vivo*. A. FGG overexpression was performed with MCF7 and T47D cells. FGG protein levels of infected human breast cancer cells were measured with Western blot assays. β -actin was used as loading control. B. MCF7-FGG/-vector cells were treated with a gradient concentration of EPI. CCK-8 assays were performed to determine the IC₅₀ of infected cells, which was analyzed with a nonlinear regression model with GraphPad Prism. C and D. Cell viability was measured in MCF7-FGG and T47D-FGG cells and control with 3.0 μ M EPI treatment for 72 hours. E. Cell clone formation assays were performed with infected MCF7 and T47D cells, which showed increased cell clones than corresponding control cells. F. Representative images of clone formation of infected MCF7 and T47D cells, which were captured after 14 days culture. G. Xenografts of infected MCF7 cells were planted and treated with EPI medium (5 mg/kg EPI once per 3 days) when the volume was about 100 mm³. Tumor volume was recorded with the mean volumes of tumor size in the indicated day. H. Xenografts were harvested and imaged after 15 days treatment. Bar = 1 cm. The tumor weights were compared between two groups. Data represent the means \pm SD. * $P < 0.05$.

cells, as evidenced by decreased cell viability in combined treatment with EPI and TMP (100 μ M) (**Figure 3B**). However, no significant inhibition of cell viability was observed in only TMP treated MCF7/EP cells (**Figure S1A**). Flow cytometry analysis was further performed to measure the percentage of apoptotic cells with TMP treatment. Compared to vehicle control group, TMP treatment significantly increased early and late apoptosis percentages of MCF7/EP cells ($P < 0.01$, **Figure 3C, 3D**). Correspondingly, increased activities of caspase 3 were observed in combined EPI and TMP treated MCF7/EP cells ($P < 0.01$, **Figure 3E**). Meanwhile no significant changes were observed in only TMP treatment (**Figure S1B**). Furthermore, the pro-apoptotic effects of TMP were also indicated by the increased cleaved PARP, and decreased Bcl-2 and bcl-xl (**Figure 3F**). Next, we evaluated the therapeutic efficacy of TMP on tumor growth of breast cancer *in vivo*. MCF7/EP cells were subcutaneously implanted into six-week-old athymic nude mice in fat pad. Then, the mice were treated with TMP and EPI in an intravenous infusion (5 mg/kg). Marked inhibitory potency was observed on tumor growth in combined TMP treatment group (**Figure 3G**). The mean tumor volume and weight of TMP-treated group were both significantly lower than the control group after 15 days treatment (**Figure 3H**). Further analysis indicated that only TMP treatment failed to inhibit tumor growth *in vivo* (**Figure S1C**). Collectively, these results indi-

cated that TMP reversed anthracycline resistance of breast cancer cells.

cated that TMP reversed anthracycline resistance of breast cancer cells.

Ligustrazine reverts breast cancer anthracycline chemoresistance

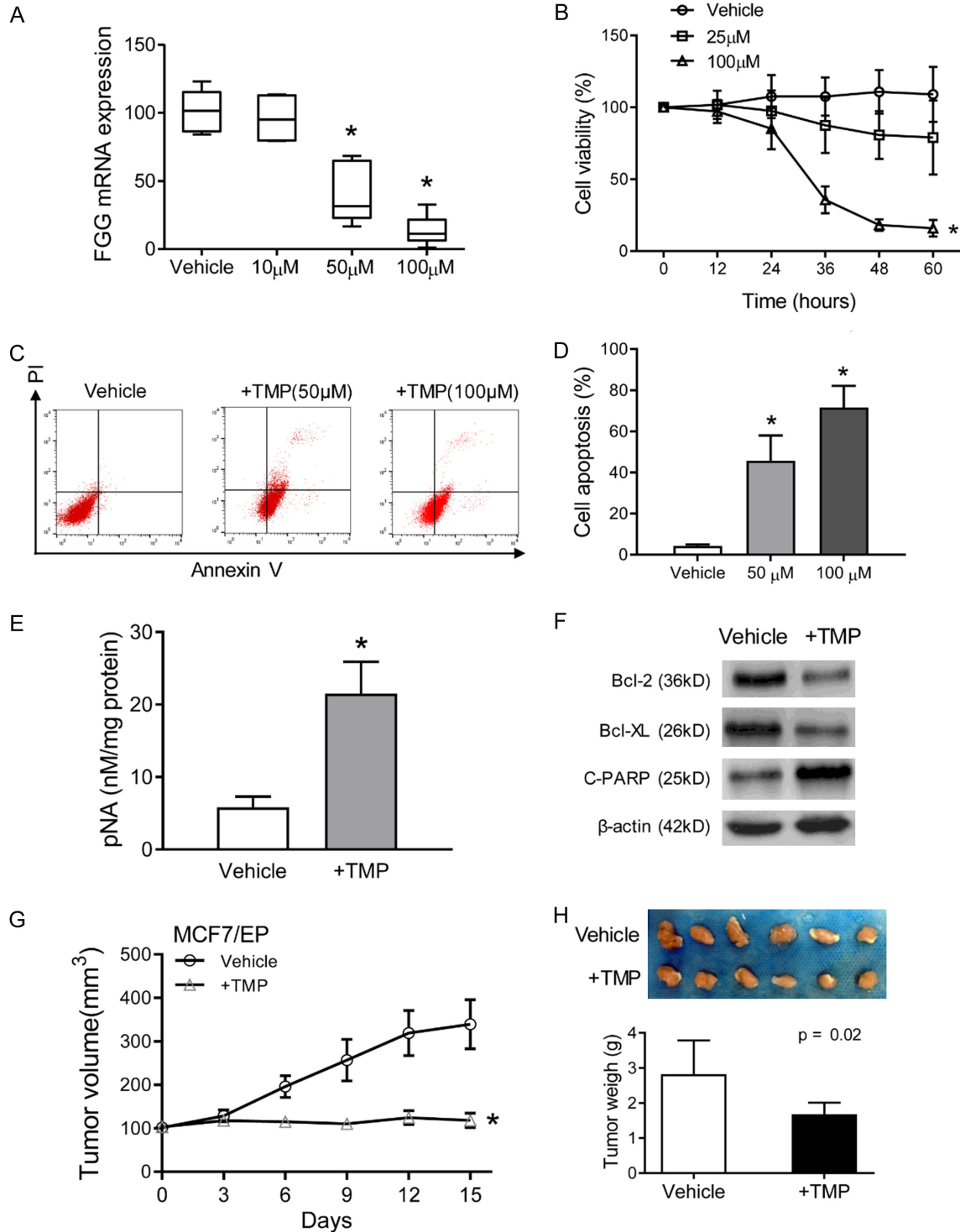


Figure 3. TMP reduces FG expression and reverses anthracycline resistance of breast cancer cells. (A) MCF7/EP cells were treated with a gradient concentration of TMP for 48 h. The mRNA levels of FG were measured with qRT-PCR assays. β -actin was used as control. (B) Cell viability of MCF7/EP cells were detected with CCK-8 assays. MCF7/EP cells were treated with combined EPI (3 μ M) and indicated concentration of TMP for 60 h. (C) MCF7/EP cell apoptosis was measured in different treatment: EPI (3 μ M) + vehicle, EPI (3 μ M) + TMP (50 or 100 μ M). Cell apoptosis was analyzed with flow cytometry by Propidium iodine and Annexin V staining. (D) Statistics of MCF7/EP cell apoptosis in combined treatment or EPI only groups as described in (C). (E) Activity of caspase-3 was measured by pNA concentrations with Caspase-3 Activity Assay Kit. (F) Apoptosis related proteins (cleaved PARP, Bcl-2 and Bcl-XL) in TMP treated MCF7/EP cells were analyzed with Western blot assays. β -actin was used as loading control. (G) Xenografts growth of MCF7/EP cells with the treatment of EPI with/without TMP. Tumor volume was recorded after

Ligustrazine reverts breast cancer anthracycline chemoresistance

the treatment with the mean tumor volumes in the indicated day. (H) Xenografts were harvested and imaged after 15 days' treatment. The tumor weights were compared between groups. Bar = 1 cm. Data represent the means \pm SD. * $P < 0.05$.

TMP eliminates cancer stem cells of anthracycline resistant breast cancer cells

Further investigation was performed to study stemness related characteristics of TMP treated breast cancer cells. Suspended tumor spheres were established with the help of non-adhesive suspension culture system. Anthracycline resistant MCF7/EP cells, formed floating spherical colonies within 7 days, whereas TMP treatment significantly reduced the volume of mammospheres (**Figure 4A**). More importantly, decreased number of mammospheres were observed with TMP treatment (**Figure 4B**). Secondary spheroids were also cultured and calculated to confirm that TMP treatment eliminated breast cancer stem cell (**Figure 4A, 4B**). More importantly, decreased percentage of breast CSCs (ALDH1^{high}) was also observed under the condition of TMP treatment by flowcytometry analysis (**Figure 4C**). Next, FACS sorted ALDH1^{high} cells were treated with different concentrations of TMP for 48 h, indicating TMP inhibited the proliferation of breast CSCs (ALDH1^{high} cells subpopulation) (**Figure 4D**). Next, we evaluated the effect of TMP on tumorigenesis of breast cancer *in vivo*. MCF7/EP cells were treated with TMP or vehicle for 48 hours, then dissociated and implanted subcutaneously into the fat pad of nude mice. The results showed decreased tumorigenicity of TMP treated cells than control cells (**Figure 4E, 4F**). Furthermore, IHC staining was performed with the xenografts of TMP treated MCF7/EP cells, and the results showed that TMP treatment decreased bcl-2, ki67, ALDH1A1 and p-STAT3 expression in xenografts (**Figure 4G**). Taken together, these data suggest that TMP is an effective agent in inhibiting self-renewal capacity of breast cancer cells.

TMP reduces FG expression by JAK2/STAT3 pathway inhibition in breast cancer cells

Based on the above results, we studied the underlying mechanism of TMP in reversing EPI resistance. CCK8 assays showed that combined treatment of TMP did not increase the toxicity of EPI for MCF7-FGG cells (**Figure 5A**). Moreover, there is no significant change in the percentage of ALDH1^{high} cells in FGG overex-

pressing patients under TMP treatment (**Figure 5B**). These results supported a crucial role of FGG in synergistic effects of TMP in EPI based chemotherapy of breast cancer.

Previous studies indicated that EPI resistant was correlated with JAK2/STAT3 signal activation [16]. We explored their correlation with elevated FGG expression in anthracycline-resistant breast cancer cells. Immunoblotting assays were performed for the status of JAK2/STAT3 signal activation of TMP treated MCF7/EP cells, and the results showed that STAT3 and JAK2 phosphorylation and Oncostatin M level was increased in EPI treated MCF7/EP cells, whereas 50 μ M TMP treatment decreased their expression (**Figure 5C**). However, we did not observe significant change in STAT3 and JAK2 phosphorylation levels between FGG overexpressing cells and corresponding control (**Figure 5D**). Therefore, these results suggested that TMP inhibited JAK2/STAT3 signaling to decrease FGG expression.

To further confirm the role of STAT3 activation in FGG regulation, parental MCF7 cells were infected with a constitutively activated STAT3 construct (STAT3-C). Immunoblotting assays showed increased FGG protein level in STAT3-C infected cells, which was also not attenuated with TMP treatment (**Figure 5E**). Flowcytometry assays showed that combined EPI and TMP treatment failed to enhance cell apoptosis of MCF7-STAT3-C cells (**Figure 5F, 5G**). Moreover, STAT3-C-overexpressing cells also significantly abrogated cell proliferation inhibition effects of TMP treatment, which was confirmed with CCK-8 assays (**Figure 5H**). These results supported that JAK2/STAT3 signaling inhibition is involved in TMP treatment induced FGG down-regulation. JAK2/STAT3 blockage by TMP was a valuable chemosensitizer for breast cancer therapy.

Elevated FG expression in tumor tissue predicts poor survival estimation of breast cancer

IHC staining for FGG was performed with 405 breast cancer specimens. Positive FGG expression was detected in 42 breast cancer specimens (56.76%), which was arranged in cytoplasm and tumor stroma (**Figure 6A**). Notably,

Ligustrazine reverts breast cancer anthracycline chemoresistance

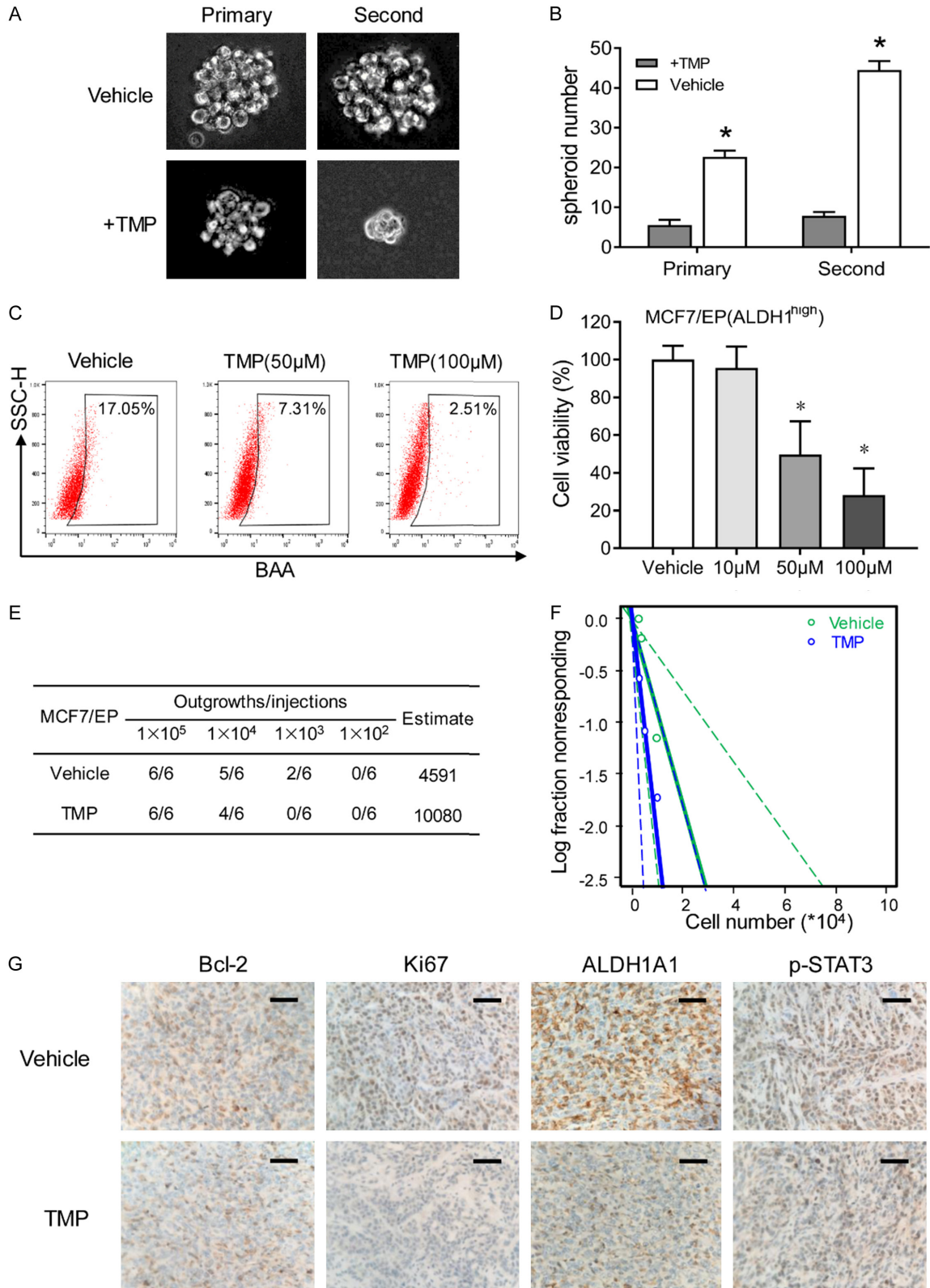
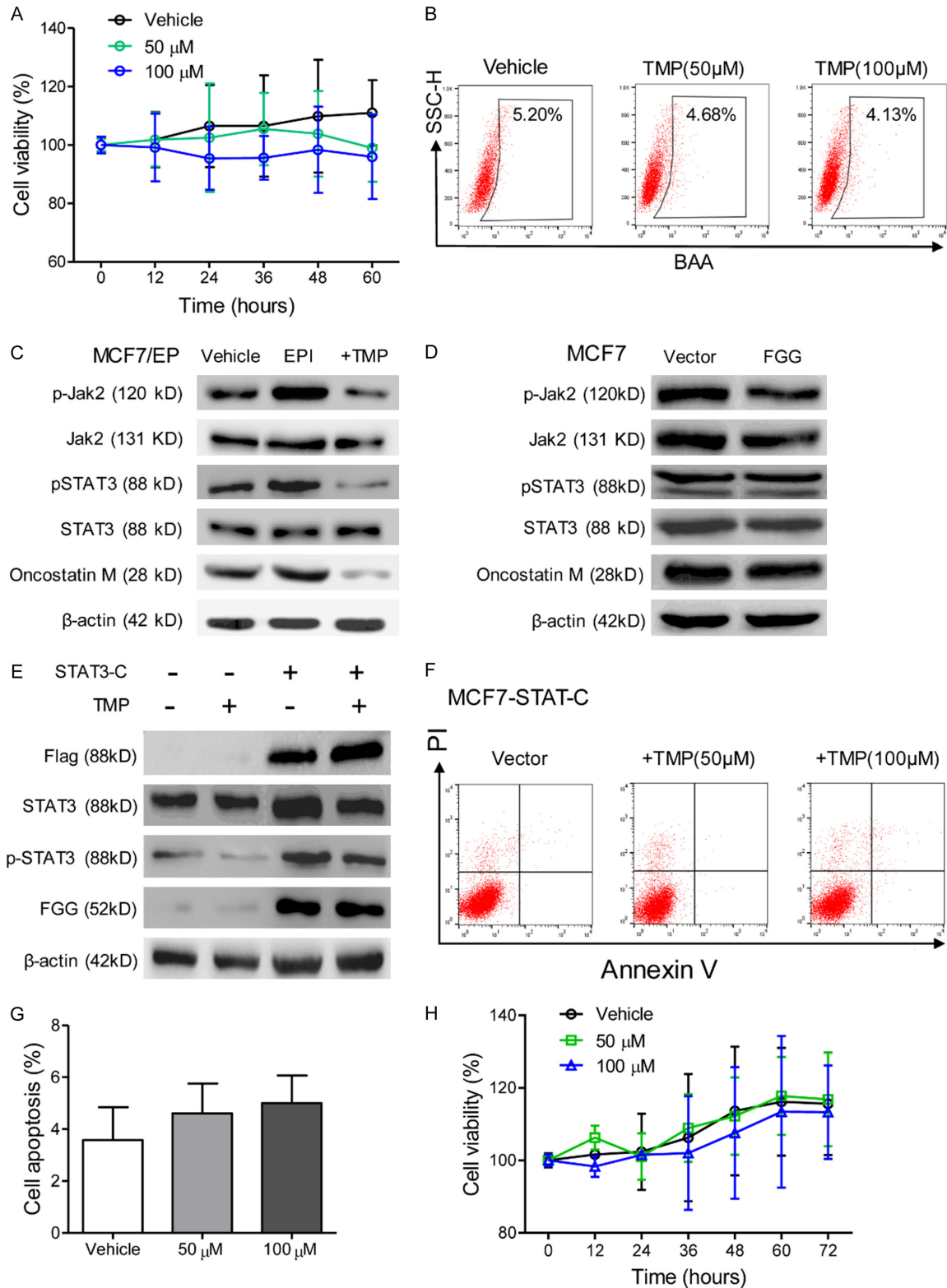


Figure 4. TMP eliminates cancer stem cells of anthracycline resistant breast cancer cells. A. Single MCF7/EP cells were consecutively planted in suspension culture system, which were treated with 50 µM TMP for 7 days. Representative images of mammospheres were captured at the 7th day. B. Mammosphere number was counted and compared between different groups at the 7th day. C. MCF7/EP cells was treated with different concentration of TMP for 48 h. Flowcytometry analysis was performed for the ALDH1^{high} percentage of the cells with different treatment. D. MCF7/EP-ALDH1^{high} cells were sorted for cell viability inhibition analysis. FACS sorted cells were treated

Ligustrazine reverts breast cancer anthracycline chemoresistance

with combined EPI and indicated concentration of TMP for 48 h. Data represent the means \pm SD. * $P < 0.01$. E and F. MCF7/EP cells were treated with combined EPI and TMP (50 μ M) or only EPI for 48 hours. Serial dilution of cells were implanted into the mammary fat pads of nude mice for xenografts (n = 6 each group). Tumor initiation numbers were analyzed with Extreme Limiting Dilution Analysis. G. IHC staining of Bcl-2, Ki67, ALDH1A1 and p-STAT3 were performed with the xenografts of TMP treated MCF7/EP cells. Scale bars, 20 μ m.



Ligustrazine reverts breast cancer anthracycline chemoresistance

Figure 5. TMP reduces FGG expression by JAK2/STAT3 pathway inhibition in breast cancer cells. (A) Cell viability of MCF7-FGG cells with combined treatment of EPI and TMP were tested with CCK-8 assays for 60 h. (B) Flowcytometry analysis of the percentage of ALDH1^{high} in MCF7-FGG cells which was treated with TMP (0, 50, 100 μ M) for 48 h. (C) Western blot assays were performed for the expression of phosphorylated JAK2 and STAT3, Oncostatin M, in vehicle, EPI or EPI+TMP treated MCF7/EP cells for 48 hours. (D) MCF7-FGG/-Vector cells were treated with 3.0 μ M EPI for 48 hours. Western blot assays were performed for the expression of phosphorylated JAK2 and STAT3, Oncostatin M. (E) MCF7 cells were infected with a constitutively activated STAT3 (STAT3-C). Western blot assays were performed for FGG expression in the cells which were treated with EPI or combined with TMP (50 μ M). β -actin was used as loading control. (F) Flowcytometry assays showed that STAT3-C effectively rescued MCF7 cells with combined TMP and EPI treatment. (G) Cell apoptosis was compared among different treatment groups as described in (F). (H) Cell proliferation of STAT3-C infected cells was measured with CCK-8 assays, which was treated with combined EPI and TMP. Data represent the means \pm SD from three independent experiments. *P < 0.05.

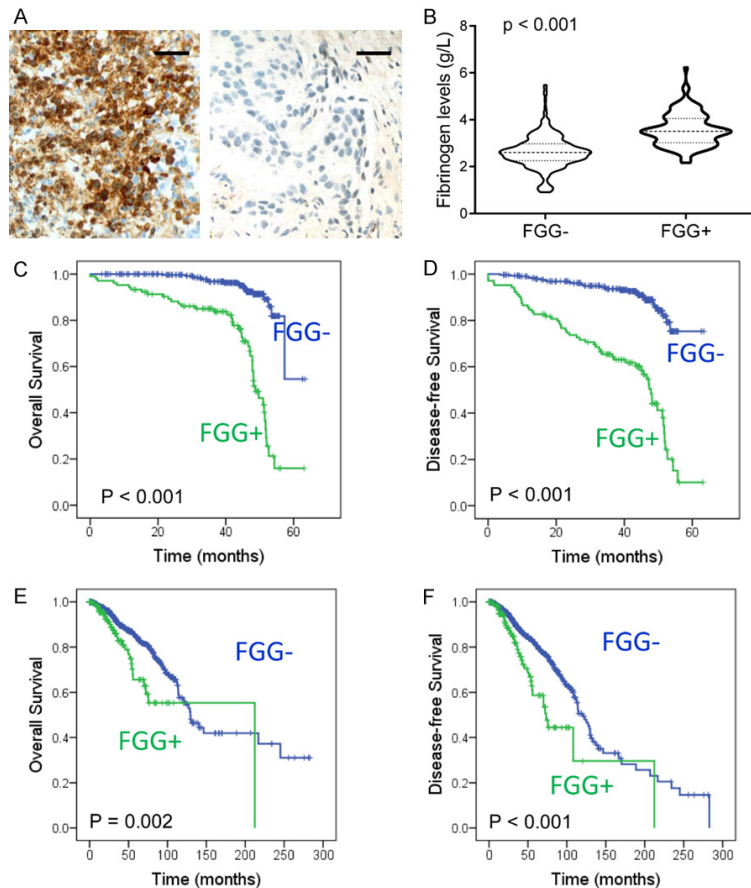


Figure 6. Elevated FGG expression correlates with poor prognosis of breast cancer. A. Immunohistochemical staining of FGG in breast cancer tissues. Representative IHC staining images of FGG were shown. Bar, 100 μ m. B. The plasma fibrinogen levels were compared between FGG positive patients and negative ones. C and D. Kaplan-Meier analysis showed significant worse overall survival and disease-free survival in FGG positive patients than negative ones (P < 0.001 respectively). E and F. Kaplan-Meier analysis showed significant worse overall survival and disease-free survival in FGG mRNA positive patients than negative ones with TCGA data (P = 0.002 and P < 0.001, respectively).

increased serum fibrinogen levels were observed in FGG positive group than negative ones (**Figure 6B**). Further analysis indicated a posi-

tive correlation between FGG expression and lymph node metastasis (P < 0.001) and elevated histological grade (P < 0.001) (**Table 1**). However, no significant correlation was observed between FGG expression and other clinical variables, including age, tumor location, clinical stage and the expression of ER, PR, HER2 (P > 0.05, **Table 1**).

The median followed-up period of the patients in this study was 39.94 months (range: 1.64-63.39 months). Disease progression was observed in 88 patients (21.73%) during followup periods. Kaplan-Meier analysis showed significantly worse overall survival (OS) and disease-free survival (DFS) in FGG positive group than negative one (P < 0.001, respectively, **Figure 6C, 6D**). Cox regression analysis also indicated an independent prognostic significance of FGG with univariate analysis (OS: HR = 7.137, 95% CI: 4.196-12.141, P < 0.001; DFS: HR = 6.080, 95% CI: 3.932-9.401, P < 0.001, **Table 2**). Multivariate analysis also showed that FGG expression was a detrimental factor for both OS and DFS (OS: HR = 8.641, 95% CI: 4.738-15.758, P < 0.001; DFS:

HR = 5.862, 95% CI: 3.566-9.634, P < 0.001. **Table 2**). Furthermore, Kaplan-Meier analysis of TCGA breast cases also supported that ele-

Ligustrazine reverts breast cancer anthracycline chemoresistance

Table 1. Relationship between Clinical Characteristics and FGG Expression

Characteristic	Number (%)	FGG expression		p value
		Positive	Negative	
Total	405	104 (25.7%)	301 (74.3%)	
Age, years				
< 50	241 (59.5%)	59 (14.6%)	182 (44.9%)	0.563
≥ 50	164 (40.5%)	45 (11.1%)	119 (29.4%)	
Tumor size, cm				
≤ 2	167 (41.2%)	45 (11.1%)	122 (30.1%)	0.394
2-5	202 (49.9%)	47 (11.6%)	155 (38.3%)	
≥ 5	36 (8.9%)	12 (3.0%)	24 (5.9%)	
Histological status				
I	122 (30.1%)	14 (3.5%)	108 (26.7%)	< 0.001
II	184 (45.4%)	37 (9.1%)	147 (36.3%)	
III	99 (24.4%)	53 (13.1%)	46 (11.4%)	
Lymph node status				
0	229 (56.5%)	28 (6.9%)	201 (49.6%)	< 0.001
1-3	107 (26.4%)	29 (7.2%)	78 (19.3%)	
≥ 4	69 (17.0%)	47 (11.6%)	22 (5.4%)	
ER				
Positive	253 (62.5%)	63 (15.6%)	190 (46.9%)	0.641
Negative	152 (37.5%)	41 (10.1%)	111 (27.4%)	
PR				
Positive	311 (76.8%)	52 (12.8%)	159 (39.3%)	0.650
Negative	194 (47.9%)	52 (12.8%)	142 (35.1%)	
HER2				
Positive	104 (25.7%)	26 (6.4%)	78 (19.3%)	0.897
Negative	301 (74.3%)	78 (19.3%)	223 (55.1%)	

Table 2. Univariate and Multivariate Analyses of FGG expression in Disease-Free Survival and Overall Survival

Variable analysis	Overall Survival			Disease-Free Survival		
	HR	95% CI	p	HR	95% CI	p
Univariate		N = 405			N = 405	
FGG	7.137	4.196-12.141	< 0.001	6.080	3.932-9.401	< 0.001
Multivariate		N = 405			N = 405	
Age	0.854	0.494-1.478	0.573	1.063	0.683-1.656	0.786
Size	1.221	0.664-2.245	0.521	1.641	0.953-2.826	0.074
Stage	0.989	0.667-1.467	0.957	0.907	0.663-1.241	0.541
Grade	0.399	0.195-0.816	0.012	0.776	0.431-1.400	0.400
Lymph	1.368	0.721-2.596	0.337	1.157	0.653-2.049	0.617
ER	0.716	0.344-1.490	0.372	0.611	0.339-1.102	0.101
PR	0.848	0.424-1.694	0.640	0.769	0.437-1.355	0.364
HER2	1.132	0.616-2.080	0.690	1.040	0.683-1.656	0.786
FGG	8.641	4.738-15.758	< 0.001	5.862	3.566-9.634	< 0.001

CI = confidence interval; HR = hazard ratios. The variables were compared in the following ways: Age, ≥ 50 years vs. < 50 years; FGG expression, positive vs. negative; size, > 2 cm vs. < 2 cm; Stage, III-IV vs. I-II; Grade, G3-4 vs. G1-2; Lymph, Yes vs. no; ER, PR, HER2, yes vs. no.

vated FGG expression was correlated with poor survival estimation of breast cancer patients (OS, P = 0.002; DFS, P < 0.001. **Figure 6E, 6F**). These results indicate that FGG expression is a valuable biomarker for evaluating the prognosis of breast cancer patients.

Discussion

Based on the above results, we proposed that FGG participates in modulating anthracycline chemotherapy sensitivity of breast cancer cells. Furthermore, TMP reverted EPI resistance by suppressing JAK2/STAT3 signaling and FGG expression, as a novel chemosensitizer for anthracycline chemoresistance in breast cancer treatment.

Anthracycline is an effective drug for breast cancer treatment, which is recommended as the first-line adjuvant chemotherapy [17]. However, metastasis and recurrence because of chemotherapy resistance are still the major cause for tumor related death [18]. Therefore, it is of particular importance to determine the core genes involved in chemotherapy resistance, and to study its effect on drug susceptibility to neoadjuvant chemotherapy. In this study, we explored the function of tumor cell derived fibrinogen expression, especially FGG, and provided evidences that tumor cell derived FGG participates in anthracycline chemore-

sistance of breast cancer. Breast cancer cell with elevated FGG expression showed a survival advantage in anthracycline treatment. Further randomized controlled trials are necessary to clinically assess the optimized regimens for the cancer patients with increased fibrinogen levels.

Microenvironmental factors, such as hypercoagulable states, have been reported to influence the therapeutic response of local tumors [19, 20]. Tumor cells also participate in the formation of hypercoagulable microenvironment, including elevated fibrinogen chain expression [10]. Fibrinogen matrix acts as a reservoir for secreted growth factors to facilitate tumor growth, angiogenesis, and distant metastasis [21, 22]. Abnormal fibrinogen levels are at least partially caused by tumor cells in local microenvironment [23]. In our previous study, we found that serum fibrinogen levels were correlated with poor response to Trastuzumab treatment in breast cancer patients [24]. Here, imbalances in the intracellular levels of different fibrinogen chains, α , β and γ chains, were also observed in tumor cells, which was consistent with hepatocytes and hepatoma cells as previous reports [25]. Aberrant FGG expression was observed in a large proportion of breast cancer specimens. In particular, an excess amount of FGG expression was identified in tumor cells and plasma under anthracycline chemoresistance. Elevated FGG expression in cancerous tissues induces chemoresistance of breast cancer. We performed clinical analysis to study the prognostic role of FGG in chemotherapy and survival estimation. We identified FGG expression in tumors was an independent detrimental factor for breast cancer patients. Other study indicated a significant correlation between FGG and C-reaction protein [26], indicating its potential function in inflammation [27]. Further analysis is still needed for the function of microenvironment in breast cancer progression, including fibrinogen-dependent inflammatory response in chemotherapy resistance.

Accumulated evidences supported that traditional Chinese medicine was an inexhaustible novel drug treasure. TMP is a major bioactive component of traditional Chinese medicine *Rhizoma Chuanxiong*, which has been widely used in cardiovascular and cerebrovascular diseases management [15, 28]. Recent studies also indicated its anticancer activity on melanoma metastasis and angiogenesis [5].

Increased tumor cell apoptosis was observed in TMP treated cells, especially multidrug resistant malignant cells [29, 30]. We found that the introduction of TMP to anthracycline increased chemotherapy cytotoxicity. More importantly, TMP reverted EPI resistance of breast cancer. Our results supported TMP as a compound to enhance the chemotherapy efficiency [31, 32].

Previous studies indicated that TMP increased intracellular reactive oxygen species accumulation to enhance tumor cell apoptosis [33]. Furthermore, TMP inhibited ATP-binding cassette transporter to revert multidrug resistance [34, 35]. In this study, we provided evidence that JAK2/STAT3 signaling activation and elevated FGG expression also participated in EPI resistance. JAK2/STAT3 signaling activation plays an important role in fundamental cellular processes, including tumorigenesis, cell proliferation and therapeutic resistance [36-38]. Especially, aberrant STAT3 signaling activation was observed in EPI resistant breast cancer cells [39, 40]. Disruption of STAT3 signaling by TMP reduced FGG expression and viability of EPI resistant cancer cells. Notably, JAK2/STAT3 inhibition by TMP supported a crucial role of this pathway for stemness maintaining of cancer stem cells [30]. Our results supported TMP as a chemosensitizer for breast cancer chemotherapy, especially anthracycline based chemotherapy. Unfortunately, the toxicity of TMP showed cumulative effects *in vivo* to some extent [15]. Thus, further modification of TMP is still needed to improve its therapeutic potency.

In conclusion, our study collectively identified FGG was an independent detrimental factor for anthracycline based chemotherapy in breast cancer patients. TMP is a novel chemosensitizer for FGG-induced anthracycline chemoresistance in breast cancer treatment.

Acknowledgements

This research was supported by grants from National Natural Science Foundation of China (81502283, 81972793), Shinan District Science and Technology Plan, Qingdao (2016-3-020-YY and 2018-4-026-YY), Shandong province Medical Health Science and Technology Project (2018WS447), Qingdao Science and Technology Program for Benefiting People Special Project 2019 (19-6-1-25-nsh), 2019 Annual Medical Scientific Research Guidance Plan of Qingdao (2019-WJZD170).

Disclosure of conflict of interest

None.

Abbreviations

EPI, Epirubicin; TMP, Ligustrazine (2,3,5,6-tetramethylpyrazine); FGG, fibrinogen gamma chain; JAK, Janus kinase; STAT, signal transducer and activator of transcription; ATCC, American Type Culture Collection; CCK-8, Cell counting Kit-8; qRT-PCR, Quantitative real-time RT-PCR; IHC, Immunohistochemistry; SD, standard deviation; STAT3-C, constitutively activated STAT3; OS, Overall survival; DFS, Disease-Free Survival; ER, estrogen receptor; PR, progesterone receptor; HER2, Human epidermal growth factor receptor 2; CI, confidence interval; HR, hazard ratios.

Address correspondence to: Jing-Wang Bi and Qiang Wang, Department of Oncology, 960 Hospital of PLA, 25# Shifan Road, Tianqiao District, Jinan 250031, China. E-mail: jingwangbi@outlook.com (JWB); wangqiang401@gmail.com (QW)

References

- [1] Siegel RL, Miller KD and Jemal A. Cancer statistics, 2018. *CA Cancer J Clin* 2018; 68: 7-30.
- [2] Paridaens R, Dirix L, Dumez H, Prove A, Wildiers H, Alvarez A, Oliveira CT, Latz J, Simms L and Melemed A. Phase I/II pharmacokinetic study of pemetrexed and epirubicin in patients with locally advanced or metastatic breast cancer. *Clin Breast Cancer* 2007; 7: 861-866.
- [3] Holohan C, Van Schaeybroeck S, Longley DB and Johnston PG. Cancer drug resistance: an evolving paradigm. *Nat Rev Cancer* 2013; 13: 714-726.
- [4] Chang CY, Kao TK, Chen WY, Ou YC, Li JR, Liao SL, Raung SL and Chen CJ. Tetramethylpyrazine inhibits neutrophil activation following permanent cerebral ischemia in rats. *Biochem Biophys Res Commun* 2015; 463: 421-427.
- [5] Chen L, Lu Y, Wu JM, Xu B, Zhang LJ, Gao M, Zheng SZ, Wang AY, Zhang CB, Zhang WW and Lei N. Ligustrazine inhibits B16F10 melanoma metastasis and suppresses angiogenesis induced by vascular endothelial growth factor. *Biochem Biophys Res Commun* 2009; 386: 374-379.
- [6] Ali BH, Al-Moundhri M, Eldin MT, Nemmar A, Al-Siyabi S and Annamalai K. Amelioration of cisplatin-induced nephrotoxicity in rats by tetramethylpyrazine, a major constituent of the Chinese herb *Ligusticum wallichii*. *Exp Biol Med (Maywood)* 2008; 233: 891-896.
- [7] Pan J, Shang JF, Jiang GQ and Yang ZX. Ligustrazine induces apoptosis of breast cancer cells in vitro and in vivo. *J Cancer Res Ther* 2015; 11: 454-458.
- [8] Palumbo JS and Degen JL. Mechanisms coupling the hemostatic system to colitis-associated cancer. *Thromb Res* 2010; 125 Suppl 2: S39-43.
- [9] Honda KI, Asada R, Kageyama K, Fukuda T, Terada H, Yasui T, Sumi T, Koyama M, Ishiko O and Sugawa T. Protein complex of fibrinogen gamma chain and complement factor H in ovarian cancer patient plasma. *Anticancer Res* 2017; 37: 2861-2866.
- [10] Perisanidis C, Psyrris A, Cohen EE, Engelmann J, Heinze G, Perisanidis B, Stift A, Filipits M, Kornek G and Nkenke E. Prognostic role of pre-treatment plasma fibrinogen in patients with solid tumors: a systematic review and meta-analysis. *Cancer Treat Rev* 2015; 41: 960-970.
- [11] Wang L, Zeng H, Wang Q, Zhao Z, Boyer TG, Bian X and Xu W. MED12 methylation by CARM1 sensitizes human breast cancer cells to chemotherapy drugs. *Sci Adv* 2015; 1: e1500463.
- [12] Zhou K, Rao J, Zhou ZH, Yao XH, Wu F, Yang J, Yang L, Zhang X, Cui YH, Bian XW, Shi Y and Ping YF. RAC1-GTP promotes epithelial-mesenchymal transition and invasion of colorectal cancer by activation of STAT3. *Lab Invest* 2018; 98: 989-998.
- [13] Wang Q, Jiang J, Ying G, Xie XQ, Zhang X, Xu W, Zhang X, Song E, Bu H, Ping YF, Yao XH, Wang B, Xu S, Yan ZX, Tai Y, Hu B, Qi X, Wang YX, He ZC, Wang Y, Wang JM, Cui YH, Chen F, Meng K, Wang Z and Bian XW. Tamoxifen enhances stemness and promotes metastasis of ERalpha36(+) breast cancer by upregulating ALDH1A1 in cancer cells. *Cell Res* 2018; 28: 336-358.
- [14] Wang Q, Shi YL, Zhou K, Wang LL, Yan ZX, Liu YL, Xu LL, Zhao SW, Chu HL, Shi TT, Ma QH and Bi J. PIK3CA mutations confer resistance to first-line chemotherapy in colorectal cancer. *Cell Death Dis* 2018; 9: 739.
- [15] Chen H, Li G, Zhan P and Liu X. Ligustrazine derivatives. Part 5: design, synthesis and biological evaluation of novel ligustrazinyloxy-cinnamic acid derivatives as potent cardiovascular agents. *Eur J Med Chem* 2011; 46: 5609-5615.
- [16] Zhang W, Qiao B and Fan J. Overexpression of miR-4443 promotes the resistance of non-small cell lung cancer cells to epirubicin by targeting INPP4A and regulating the activation of JAK2/STAT3 pathway. *Pharmazie* 2018; 73: 386-392.
- [17] Telli ML, Gradishar WJ and Ward JH. NCCN guidelines updates: breast cancer. *J Natl Compr Canc Netw* 2019; 17: 552-555.
- [18] Calaf GM, Zepeda AB, Castillo RL, Figueroa CA, Arias C, Figueroa E and Farias JG. Molecular

- aspects of breast cancer resistance to drugs (Review). *Int J Oncol* 2015; 47: 437-445.
- [19] Bustin SA, Benes V, Garson JA, Hellemans J, Huggett J, Kubista M, Mueller R, Nolan T, Pfaffl MW, Shipley GL, Vandesompele J and Wittwer CT. The MIQE guidelines: minimum information for publication of quantitative real-time PCR experiments. *Clin Chem* 2009; 55: 611-622.
- [20] Dean JL, McClendon AK, Hickey TE, Butler LM, Tilley WD, Witkiewicz AK and Knudsen ES. Therapeutic response to CDK4/6 inhibition in breast cancer defined by ex vivo analyses of human tumors. *Cell Cycle* 2012; 11: 2756-2761.
- [21] Martino MM, Briquez PS, Ranga A, Lutolf MP and Hubbell JA. Heparin-binding domain of fibrin(ogen) binds growth factors and promotes tissue repair when incorporated within a synthetic matrix. *Proc Natl Acad Sci U S A* 2013; 110: 4563-4568.
- [22] Witsch E, Sela M and Yarden Y. Roles for growth factors in cancer progression. *Physiology (Bethesda)* 2010; 25: 85-101.
- [23] Diao D, Wang Z, Cheng Y, Zhang H, Guo Q, Song Y, Zhu K, Li K, Liu D and Dang C. D-dimer: not just an indicator of venous thrombosis but a predictor of asymptomatic hematogenous metastasis in gastric cancer patients. *PLoS One* 2014; 9: e101125.
- [24] Liu YL, Lu Q, Liang JW, Xia Y, Zhang W, Hu BQ, Shang FF, Ji YR, Wang J, Wang Q and Liang B. High plasma fibrinogen is correlated with poor response to trastuzumab treatment in HER2 positive breast cancer. *Medicine (Baltimore)* 2015; 94: e481.
- [25] Zhu WL, Fan BL, Liu DL and Zhu WX. Abnormal expression of fibrinogen gamma (FGG) and plasma level of fibrinogen in patients with hepatocellular carcinoma. *Anticancer Res* 2009; 29: 2531-2534.
- [26] Cheung EY, Vos HL, Kruip MJ, den Hertog HM, Jukema JW and de Maat MP. Elevated fibrinogen gamma' ratio is associated with cardiovascular diseases and acute phase reaction but not with clinical outcome. *Blood* 2009; 114: 4603-4604; author reply 4604-4605.
- [27] Rein-Smith CM, Anderson NW and Farrell DH. Differential regulation of fibrinogen gamma chain splice isoforms by interleukin-6. *Thromb Res* 2013; 131: 89-93.
- [28] Lan Z, Bi KS and Chen XH. Ligustrazine attenuates elevated levels of indoxyl sulfate, kidney injury molecule-1 and clusterin in rats exposed to cadmium. *Food Chem Toxicol* 2014; 63: 62-68.
- [29] Ai Y, Zhu B, Ren C, Kang F, Li J, Huang Z, Lai Y, Peng S, Ding K, Tian J and Zhang Y. Discovery of new monocarbonyl ligustrazine-curcumin hybrids for intervention of drug-sensitive and drug-resistant lung cancer. *J Med Chem* 2016; 59: 1747-1760.
- [30] Xu B, Yan WQ, Xu X, Wu GR, Zhang CZ, Han YT, Chu FH, Zhao R, Wang PL and Lei HM. Combination of amino acid/dipeptide with ligustrazine-betulinic acid as antitumor agents. *Eur J Med Chem* 2017; 130: 26-38.
- [31] Xu B, Chu F, Zhang Y, Wang X, Li Q, Liu W, Xu X, Xing Y, Chen J, Wang P and Lei H. A series of new ligustrazine-triterpenes derivatives as anti-tumor agents: design, synthesis, and biological evaluation. *Int J Mol Sci* 2015; 16: 21035-21055.
- [32] Chu F, Xu X, Li G, Gu S, Xu K, Gong Y, Xu B, Wang M, Zhang H, Zhang Y, Wang P and Lei H. Amino acid derivatives of ligustrazine-oleanolic acid as new cytotoxic agents. *Molecules* 2014; 19: 18215-18231.
- [33] Yi B, Liu D, He M, Li Q, Liu T and Shao J. Role of the ROS/AMPK signaling pathway in tetramethylpyrazine-induced apoptosis in gastric cancer cells. *Oncol Lett* 2013; 6: 583-589.
- [34] Zhang Y, Liu X, Zuo T, Liu Y and Zhang JH. Tetramethylpyrazine reverses multidrug resistance in breast cancer cells through regulating the expression and function of P-glycoprotein. *Med Oncol* 2012; 29: 534-538.
- [35] Wang XB, Wang SS, Zhang QF, Liu M, Li HL, Liu Y, Wang JN, Zheng F, Guo LY and Xiang JZ. Inhibition of tetramethylpyrazine on P-gp, MRP2, MRP3 and MRP5 in multidrug resistant human hepatocellular carcinoma cells. *Oncol Rep* 2010; 23: 211-215.
- [36] Chua PJ, Lim JP, Guo TT, Khanna P, Hu Q, Bay BH and Baeg GH. Y-box binding protein-1 and STAT3 independently regulate ATP-binding cassette transporters in the chemoresistance of gastric cancer cells. *Int J Oncol* 2018; 53: 2579-2589.
- [37] Wang Z, Si X, Xu A, Meng X, Gao S, Qi Y, Zhu L, Li T, Li W and Dong L. Activation of STAT3 in human gastric cancer cells via interleukin (IL)-6-type cytokine signaling correlates with clinical implications. *PLoS One* 2013; 8: e75788.
- [38] Kiu H and Nicholson SE. Biology and significance of the JAK/STAT signalling pathways. *Growth Factors* 2012; 30: 88-106.
- [39] Sun WL, Wang L, Luo J, Zhu HW and Cai ZW. Ambra1 modulates the sensitivity of breast cancer cells to epirubicin by regulating autophagy via ATG12. *Cancer Sci* 2018; 109: 3129-3138.
- [40] Zhang F, Wang Z, Fan Y, Xu Q, Ji W, Tian R and Niu R. Elevated STAT3 signaling-mediated up-regulation of MMP-2/9 confers enhanced invasion ability in multidrug-resistant breast cancer cells. *Int J Mol Sci* 2015; 16: 24772-24790.

Ligustrazine reverts breast cancer anthracycline chemoresistance

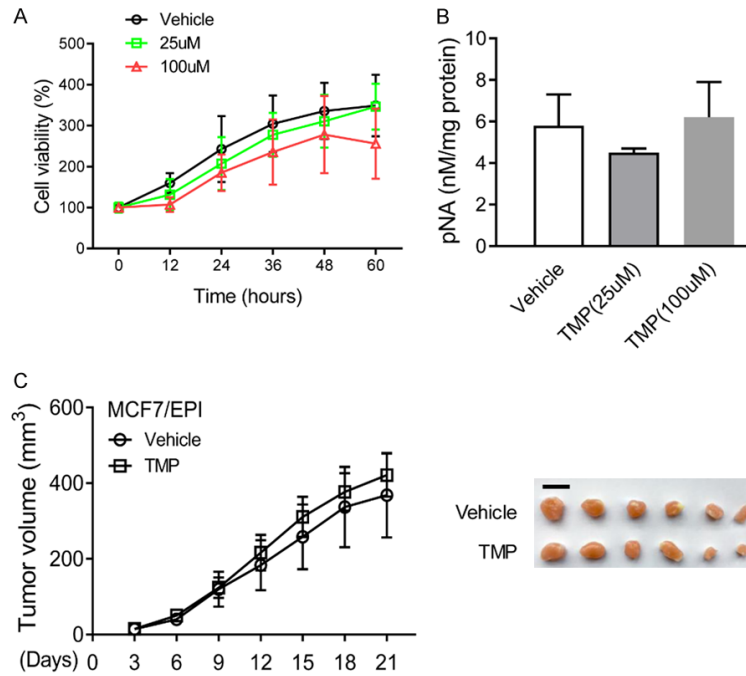


Figure S1. TMP treatment in anthracycline resistant breast cancer cells. A. Cell viability of MCF7/EP cells were detected with CCK-8 assays. MCF7/EP cells were treated with vehicle or indicated concentration of TMP for 60 h. B. Activity of caspase-3 was measured by pNA concentrations with Caspase-3 Activity Assay Kit. C. Xenografts growth of MCF7/EP cells with the treatment of vehicle or TMP. Tumor volume was recorded after the treatment with the mean tumor volumes in the indicated day. Xenografts were harvested and imaged after 21 days' treatment. Bar = 1 cm. Data represent the means \pm SD.